

Visualizing CTL activity for different CD8⁺ effector T cells supports the idea that lower TCR/epitope avidity may be advantageous for target cell killing

MR Jenkins^{1,5}, NL La Gruta¹, PC Doherty^{1,2}, JA Trapani³, SJ Turner^{*1} and NJ Waterhouse⁴

Time-lapse video microscopy allows analysis of the interaction between individual CTLs and adherent peptide-pulsed targets, from contact, to lymphocyte detachment, APC rounding, phosphatidylserine exposure and finally loss of plasma membrane integrity characteristic of end-stage apoptosis. Using *in vitro*-stimulated effectors specific for the ovalbumin K^bOVA₂₅₇ (OT-I) and influenza A virus D^bNP₃₆₆ and D^bPA₂₂₄ epitopes, no significant correlation was found between the duration of CTL contact and the time to phosphatidylserine exposure or loss of membrane integrity. Furthermore, there were minimal indications that transgenic T cells specific for the K^bOVA₂₅₇ epitope (TCR) diversity had any effect. However, when the analysis was repeated with D^bNP₃₆₆ and D^bPA₂₂₄-specific CTLs recovered directly from the lungs of mice with influenza pneumonia, the lower avidity D^bNP₃₆₆-specific set was found to elute much more quickly. Shorter contact time may allow individual CTLs to lyse more targets, suggesting that lower TCR/epitope avidity may be more beneficial than higher epitope avidity for cell-mediated immunity.

Cell Death and Differentiation (2009) 16, 537–542; doi:10.1038/cdd.2008.176; published online 9 January 2009

Analysis with the influenza A virus mouse pneumonia model has established that virus-specific CD8⁺ CTL activity is central to the normal operation of cell-mediated immunity and optimal virus clearance from the infected lung.¹ The classical *in vitro* correlate of such CTL function is the short-term (4–6 h) ⁵¹Cr release assay, an analytical system that is totally dependent on the capacity of the CD8⁺ effectors to express the effector molecule perforin (pfp).² Other effector molecules, including the serine proteases granzyme (grz) A and B do not appear to be essential for promoting rapid cell-mediated cytotoxicity,^{3,4} although grzB is required for the induction of 'classical' apoptosis.⁴ We have recently shown a possible compensatory role for the much less analysed grzK that features prominently (at least at the mRNA level) in the influenza A virus-specific CTL response.^{5,6}

Influenza A virus-immune CD8⁺ T cells specific for the prominent D^bNP₃₆₆ and D^bPA₂₂₄ epitopes mediate comparable levels of rapid ⁵¹Cr release from H2^b targets pulsed with the cognate peptide,⁷ and show equivalent pfp and grz mRNA expression profiles when recovered from the pneumonic lung by bronchoalveolar lavage (BAL) at the peak of the inflammatory process.⁵ However, other qualitative differences exist. For example, D^bPA₂₂₄-specific CTLs showed greater T-cell receptor repertoire diversity compared with D^bNP₃₆₆-specific CTLs.^{8,9} In addition, analysis of tetramer elution kinetics showed that the avidity of the transgenic T cells specific for the K^bOVA₂₅₇ epitope (TCR/

pMHC) interaction is higher for D^bPA₂₂₄ than for D^bNP₃₆₆.^{10,11} Importantly, the increased avidity observed for D^bPA₂₂₄-specific CTLs correlated with increased cytokine production elicited by short-term, *in vitro* peptide stimulation. This has been of particular interest because, although the number of specific CTLs are approximately equivalent in magnitude following primary infection, the D^bNP₃₆₆-specific population is (at least in the numerical sense) massively overdominant following secondary challenge.¹²

The mode of target cell death induced by activated CTLs depends on the spectrum of pfp/grz expression.^{3,4} An important implication of earlier observations is that D^bPA₂₂₄ and D^bNP₃₆₆-specific CTLs may differentially interact with target cells resulting in different modes of killing. Such differences in killing are not possible to measure using the standard *in vitro* ⁵¹Cr-release assay. The present experiments use *in vitro* time-lapse microscopy to probe the issue of TCR/epitope interaction at the level of CTL/target contact time, then the interval to completion of the lytic process for D^bNP₃₆₆- and D^bPA₂₂₄-specific effector populations. The results indicate that both D^bNP₃₆₆- and D^bPA₂₂₄-specific CTLs induce target cell death through a classical apoptosis pathway. Importantly, analysis of activated effectors recovered directly from the virus-infected lung showed that differential pMHC/TCR avidity correlated with decreased periods of CTL contact with the target cell, although this did not impact the time, or the mode, of target cell death. Interestingly, these differences

¹Department of Microbiology and Immunology, The University of Melbourne, Parkville, Victoria 3010, Australia; ²Department of Immunology, St. Jude Children's Research Hospital, Memphis, TN 38105, USA; ³Cancer Cell Death Laboratory, Peter MacCallum Cancer Centre, Locked Bag 1, A'Beckett Street, Melbourne, Victoria 3006, Australia and ⁴Apoptosis and Natural Toxicity Laboratory, Peter MacCallum Cancer Centre, Locked Bag 1, A'Beckett Street, Melbourne, Victoria 3006, Australia
*Corresponding author: SJ Turner, Department of Microbiology and Immunology, The University of Melbourne, Royal Parade, Melbourne, Victoria 3010, Australia.
Tel: +613 83448090; Fax: +613 93471540; E-mail: sjturn@unimelb.edu.au

⁵Current address: Cambridge Institute for Medical Research, University of Cambridge, Wellcome/MRC Building, Hills Road, Cambridge, UK

Keywords: apoptosis; cytotoxicity; T cells; cytotoxic; viral

Abbreviations: HK, HKx31 (H3N2) influenza A virus; NP, PA, influenza virus nucleoprotein and acid polymerase; OVA, OT-I ovalbumin; TCR, transgenic T cells specific for the K^bOVA₂₅₇ epitope; PR8, A/PR/8/34 H1N1 influenza A virus

Received 27.5.08; revised 24.10.08; accepted 30.10.08; Edited by DR Green; published online 09.1.09

were masked for very potent, *in vitro*-stimulated CTL populations. An important implication of this data is that lower pMHC/TCR avidity and shorter contact times may result in enhanced T-cell killing efficiency during infection.

Results

Characteristics of a single CTL/target interaction. First, we standardized the assay system by activating transgenic OT-I T cells that express a single TCR specific for the ovalbumin K^bOVA₂₅₇ epitope, by culturing them *in vitro* with peptide, in the presence of IL-2 (10 U/ml) for 5 days. These effector cells were then incubated with adherent MC57G (H2^b) fibroblasts that had been pulsed with 1 μ M of the OVA_{257–264} (SIINFEKL) peptide and followed the effector/target interactions by time-lapse microscopy (see Supplementary Movie 1). The analysis (Figure 1) focused on: (i) the duration of CTL/target contact, (ii) the time to target cell rounding and loss of plasma membrane asymmetry, measured by annexin V binding to exposed phosphatidylserine (AV⁺) and (iii) the interval from AV⁺ to loss of target cell plasma membrane integrity (measured by propidium iodide (PI) uptake). As illustrated in Figure 1a, motile OT-I CTL and sessile MC57G targets are readily distinguished by both their size and appearance (arrow, panel i). They remain in contact for varying times, although CTL elution does not necessarily precede the rounding-up, detachment (from plastic) and plasma membrane blebbing that signals progression to target cell death (Figure 1a, panel ii). The final stage is the total loss of membrane integrity, evidenced by PI uptake (Figure 1a, panel iii). The fluorescence intensity of both AV and PI staining relative to the maximum fluorescence yielded a mathematical measure of this characteristic progression to apoptotic cell death (Figure 1b).^{3,4}

Comparison of multiple interactions for *in vitro*-stimulated CTLs. The criterion adopted throughout these

time-lapse microscopy experiments was that only one CTL effector interacted with each peptide-pulsed target. The results presented in Figure 1 trace the kinetics of a single OT-I CTL/K^bOVA₂₅₇⁺ target interaction, whereas Figure 2a summarizes the profiles for repeated observations. The duration of contact (■) between individual K^bOVA₂₅₇-specific CTLs and OVA_{257–264}-pulsed MC57G cells ranged from 6 to 60 min (mean 14.61 ± 2.74 S.E.M.), whereas the 'execution' (rounding to PI⁺) phase (□) took 12–210 min (151.56 ± 12.95). There was no correlation between the length of contact and the time to PI uptake (compare ■ and □, Figure 2a).

When the analysis was repeated with *in vitro*-cultured, TCR-diverse, D^bNP₃₆₆- and D^bPA₂₂₄-specific CTL populations (Figure 2b and c), the profiles appeared to be broadly similar to those for the TCR-homogeneous OT-I set that had been stimulated *in vitro* under comparable conditions. The spectra for duration (min) of contact (D^bNP₃₆₆, 27.83 ± 3.59 ; D^bPA₂₂₄, 35.25 ± 5.57) and time from rounding to PI⁺ (D^bNP₃₆₆, 133.44 ± 16.94 ; D^bPA₂₂₄, 136.31 ± 21.03) also tended to reproduce the situation found for the OT-I analysis (Figure 2a). Even so, relatively more of the virus-specific CTLs remained in contact for >50 min, the values being: OT-I, 4%; D^bNP₃₆₆, 17% and D^bPA₂₂₄ 25%. The greater percentage of cells that show longer duration of binding within the D^bPA₂₂₄-specific set may reflect that, unlike the situation for the less TCR-diverse D^bNP₃₆₆-specific response, this T-cell population has been shown¹³ previously by tetramer elution to partition on the basis of higher ('best fit', large clone size) or lower ('non-canonical' TCR) avidity.

CTL effectors recovered directly *ex vivo*. Our long-term analysis of the influenza virus-specific CD8⁺ CTL response¹⁴ has concentrated on minimally manipulated, whole animal models. Thus, having established time-lapse profiles for TCR homogeneous (Figure 2a) *versus* polyclonal (Figure 2b and c) CTL populations that had been stimulated *in vitro* under comparable conditions, the next step was to

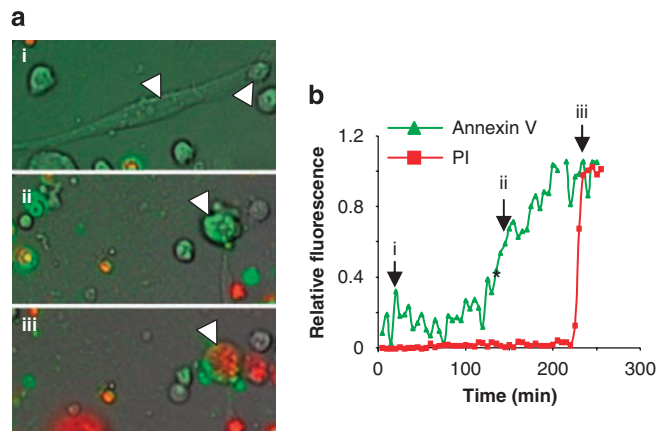


Figure 1 MC57 cells targeted by Tg OT-I CD8⁺ T cells die by apoptosis. (a) Cultured OT-I CD8⁺ T cells were overlaid on OVA₂₅₇ peptide-pulsed MC57G targets, and PI and annexin V were added to the media. Images of morphology, annexin V-Fluor and PI were then obtained every 5 min (a). The elongated MC57G target cell maintained a normal morphology (a, arrow) until 100 min, then showed rounding and blebbing by 120 min. Annexin V staining (green) was evident around these cellular protrusions (a, panel ii) by 170 min, and membrane integrity was lost (red, PI⁺) by 220 min (a, panel iii). (b) The fluorescence profiles for annexin V binding and PI relative to maximum fluorescence are presented for this individual target. The frames (a, panels i–iii) were captured at the intervals indicated by the arrows in b. The asterisk (b) denotes the 'duration of contact' to CTL disengagement from the target cell. The interval from target cell rounding to PI uptake is referred to as the 'execution phase'

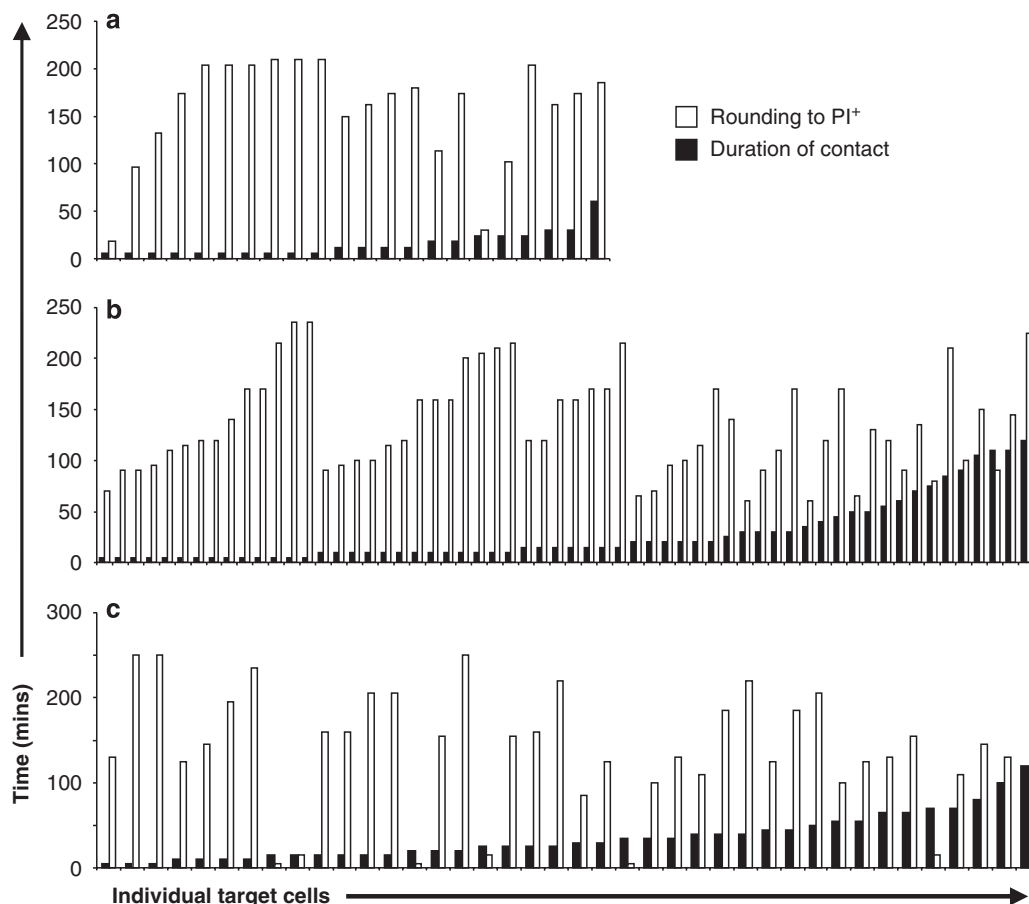


Figure 2 Profiles for multiple T-cell–target contact and execution times. *In vitro*-stimulated K^bOVA₂₅₇- (a), D^bNP₃₆₆- (b) and D^bPA₂₂₄- (c) specific CTL lines were added to adherent MC57G fibroblasts as described in the methods and images of morphology. Annexin V-FITC and PI-uptake were recorded every 5 min. The duration of CTL contact (■) and the ‘execution’ time from target cell rounding to loss of membrane potential and PI uptake (□) was assessed as illustrated in Figure 1

repeat the microscopy analysis for potent CTL effectors¹⁵ recovered directly by BAL of the virus-infected lung (Figure 3). We first examined the length of time it took for the CTLs to form a stable contact after addition to targets. Although there was a trend for the higher avidity D^bPA₂₂₄-specific cells to find and attach to a target faster (D^bPA₂₂₄ 14 ± 4 min, *n* = 11) than D^bNP₃₆₆ CTLs (25 ± 5 min, *n* = 13), this was not significant (Figure 3c). We observed that over 60% of D^bPA₂₂₄-specific CTLs remained in contact with their targets for longer than 50 min (Figure 3b), but D^bNP₃₆₆-specific CTLs did not, showing target cell contact after 50 min (Figure 3a). Interestingly, despite the higher avidity and longer duration of contacts, the D^bPA₂₂₄-specific CTLs took significantly more time to induce target cell rounding (117 ± 10 min, *n* = 11) than the D^bNP₃₆₆ CTLs (52 ± 7 min, *n* = 11) (Figure 3d and e), but there was no apparent correlation between duration of contact time and the duration of the execution phase of death duration, that is, rounding to loss of membrane integrity (Figure 3). Induction of the classical apoptosis mode of killing by activated CTLs is dependent on the pattern of pfp/grz expression.⁴ To determine if mode of killing by D^bNP₃₆₆ and D^bPA₂₂₄-specific CTLs was through classical apoptosis, D^bNP₃₆₆- and D^bPA₂₂₄-specific CTLs were cultured with

MC57G targets pulsed with 1 μM of appropriate peptide (Figure 4, Supplementary Movies 2 and 3). The morphological characteristics of target cell death (Figure 4, arrows) were measured by time-lapse microscopy as described earlier. A representative montage is shown. Target cells killed by both D^bNP₃₆₆- and D^bPA₂₂₄-specific CTLs showed morphological changes characteristic of classical apoptosis. After contact with a single CTL effector, both NP₃₆₆- and PA₂₂₄-pulsed MC57G target cells showed membrane blebbing, AV⁺ and rounding after approximately 2 h 40 min (Figure 4). Loss of membrane integrity (measure by PI uptake) occurred after 3 h from contact for both D^bNP₃₆₆- and D^bPA₂₂₄-specific CTLs. Therefore, despite observed differences in contact time (Figure 3), D^bNP₃₆₆- and D^bPA₂₂₄-specific CTLs kill target cells through classical apoptosis.

Figures 2 and 3 indicated that differences in target cell contact time between D^bNP₃₆₆- and D^bPA₂₂₄-specific CTLs was only observed directly *ex vivo*. This was confirmed by enumerating the average contact times both *in vitro*-stimulated (Figure 5a) or *ex vivo*-isolated (Figure 5b) D^bNP₃₆₆- and D^bPA₂₂₄-specific CTLs. The mean ± S.E.M. duration of target cell contact and time from initial cell rounding until death (PI⁺) are shown. The average duration of contact was not

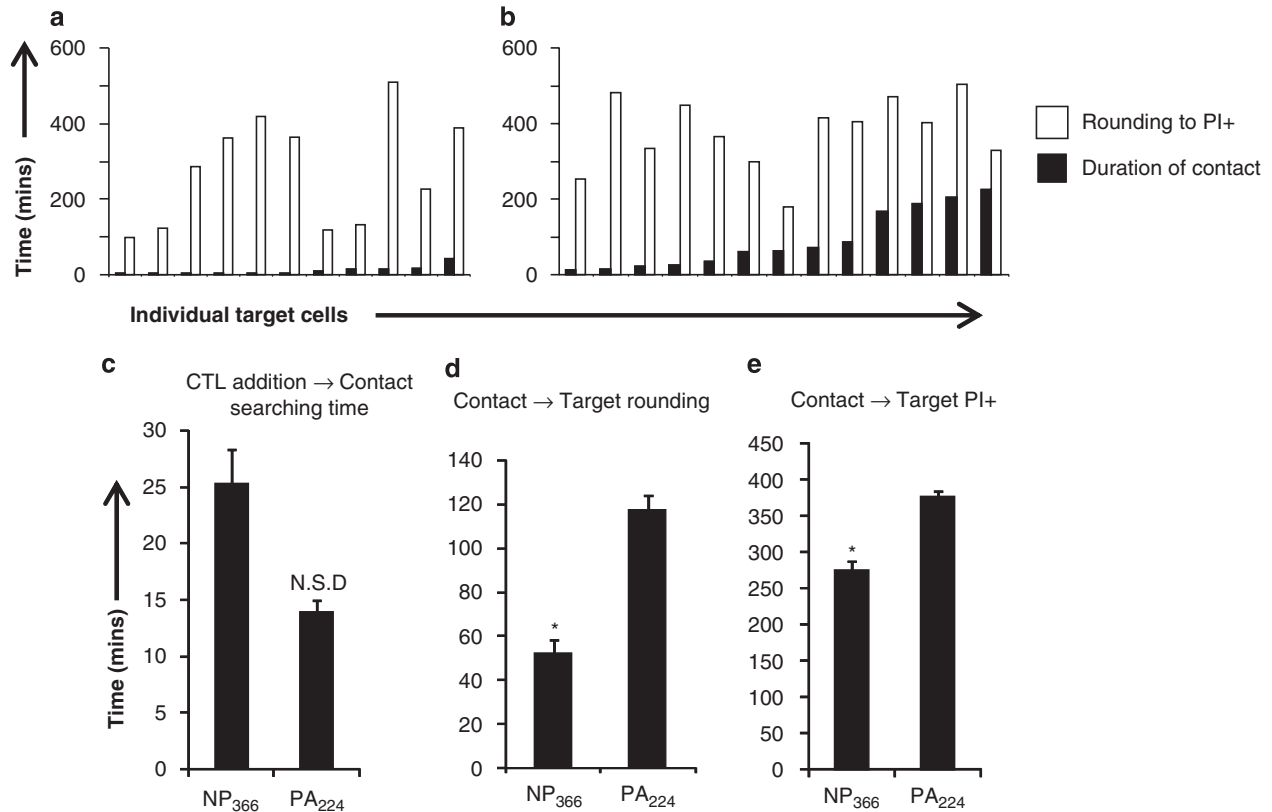


Figure 3 Interaction characteristics of the *ex vivo*-isolated CTL. Effector CD8⁺ T cells were obtained *ex vivo* by BAL of influenza virus-infected mouse lung, and added to MC57G targets pulsed previously with the NP₃₆₆ or PA₂₂₄ peptides. Images of morphology, annexin V-FLUOS and PI were obtained every 5 min to measure the duration of CTL contact (■) and the time from target cell rounding to PI uptake (□) for individual D^bNP₃₆₆- (a) and D^bPA₂₂₄- (b) specific CTL. The duration of ‘searching time’, presented as the average time (minutes ± S.E.M.) it took for the CTL to form stable contacts with targets after their addition to the assay (c), is shown. n.s.d (no statistical difference) and the time from CTL contact until target cell rounding (d) or PI+ (e) (mean minutes ± S.E.M., **P*<0.05) is shown. Data is pooled from three independent experiments

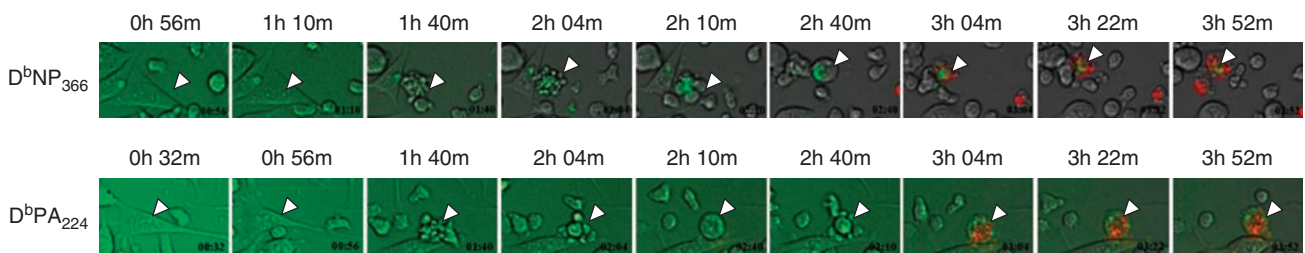


Figure 4 Montage of time-lapse microscopy of D^bNP₃₆₆- and D^bPA₂₂₄-specific CTL killing. Influenza-specific CD8⁺ T cells were isolated from the spleen of a PR8-primed mouse and further stimulated *in vitro* before adding onto MC57 target cells pulsed with NP₃₆₆ or PA₂₂₄ peptide. Images of morphology, annexin V-FLUOS and PI were obtained every 5 min. A montage of NP₃₆₆- and PA₂₂₄-specific CD8⁺ T cells mediating classical apoptosis of targets is shown here. The arrows indicate the target cell

statistically different for *in vitro*-activated D^bNP₃₆₆- and D^bPA₂₂₄-specific CTLs (Figure 5a; average 30 *versus* 40 min, respectively). In contrast, *ex vivo*-isolated D^bNP₃₆₆-specific CTLs showed significantly shorter contact time compared with D^bPA₂₂₄-specific CTLs (Figure 5b; 11 *versus* 90 min, *P*<0.05). Although *in vitro*-activated CTLs induced cell death more quickly compared with *ex vivo* CTLs, there was no difference in the time to cell death induced by either D^bNP₃₆₆- and D^bPA₂₂₄-specific CTLs (Figure 5a and b).

We have showed previously that *in vitro* culture of D^bPA₂₂₄-specific CTLs results in loss of high avidity T cells due to antigen-induced cell death.^{10,16} The loss of high-avidity

D^bPA₂₂₄ CTLs after *in vitro* stimulation was reflected in the lower proportion of CTLs that were in contact with target cells for longer than 50 min (25%, Figure 2c) when compared with *ex vivo*-isolated CTLs (61%, Figure 3b). The changes in CTL avidity were confirmed by measuring TCR/epitope avidity by tetramer elution. Although there was no obvious difference for the *in vitro*-stimulated D^bNP₃₆₆ and D^bPA₂₂₄-specific sets (Figure 5c), the D^bPA₂₂₄-specific CTLs reproduced the profile of higher avidity (Figure 5d) that has been found repeatedly¹¹ for this T-cell/epitope combination. Therefore, no difference in CTL contact time after *in vitro* peptide stimulation is most likely due to loss of high-avidity D^bPA₂₂₄-specific CTLs.

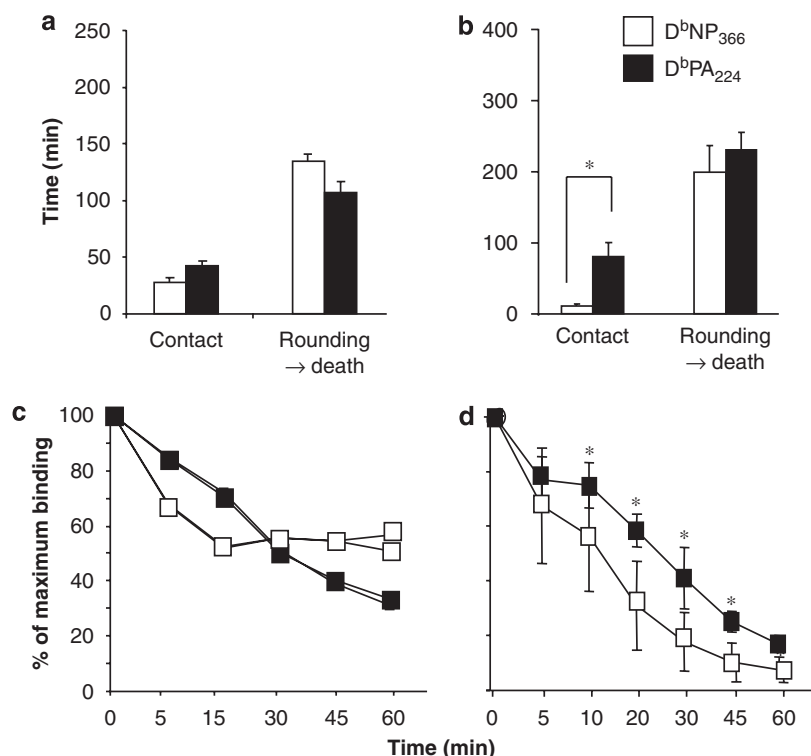


Figure 5 Summary and TCR/pMHC avidity profiles for the different CTLs. (a and b) The time intervals for: CTL/target contact, initial contact to execution (PI⁺) and target rounding to PI⁺ are presented as mean ± S.E.M. values for the *in vitro*- (a) and *in vivo* (b)-stimulated CTL populations ($n = 13$ for *ex vivo*, $n = 25$ –59 for *in vitro*). *Denotes significant differences ($P < 0.05$) between the comparable D^bNP₃₆₆- and D^bPA₂₂₄-specific sets. (c and d) Tetramer elution characteristics are shown for *in vitro* (c) and *ex vivo* (d) CTLs stained with the D^bNP₃₆₆ and D^bPA₂₂₄ tetramers (see Materials and Methods). Lymphocytes were stained with D^bNP₃₆₆ and D^bPA₂₂₄ tetramers for 1 h in the presence of H-2D^b antibody, to minimize rebinding of tetramer. The results show the % of maximum tetramer binding for: (c) the average of duplicates or (d) mean ± S.D. ($n = 5$, * $P < 0.05$)

Discussion

We have showed recently that CTL lacking grzA and B induce cell death of targets that is qualitatively different to the classical mode of apoptotic cell death typical of intact CTL.⁴ Although D^bNP₃₆₆ and D^bPA₂₂₄-specific CTL show similar cytotoxic capacity on a per cell basis,⁷ single cell analysis showed that there is heterogeneity of effector gene expression.⁵ Furthermore, these CTL populations show qualitative differences in TCR repertoire diversity,¹⁷ pMHC/TCR avidity and cytokine production.^{10,11} Therefore, it remained a formal possibility that different CTL populations may use different modes of cytotoxic killing. This study clearly shows that both *in vitro* and *ex vivo* isolated D^bNP₃₆₆- and D^bPA₂₂₄-specific CTLs induce classical apoptosis of peptide-pulsed targets, indicated by sequential annexin V⁺ and PI⁺ staining. The same mode of killing was observed also for *in vitro*-activated OT-I CTL, indicating that target cell killing through classical apoptosis is independent of TCR usage and an intrinsic property of CTLs.

The findings presented here indicate that any differences between effector CTL populations are diminished as a consequence of maximal activation following *in vitro* culture with peptide-pulsed stimulators. In agreement with previous studies,^{10,11} *ex vivo*-derived D^bPA₂₂₄-specific CTLs displayed higher avidity compared with D^bNP₃₆₆-specific CTLs, whereas no difference in avidity was observed between

in vitro-stimulated D^bNP₃₆₆- and D^bPA₂₂₄-specific CTLs. This most likely reflects loss of high-avidity D^bPA₂₂₄-specific CTLs after *in vitro* peptide stimulation due to antigen-induced cell death.¹⁶ Therefore, TCR avidity is most likely to be a major contributor to the duration of the CTL–target contact.

Interestingly, increased contact time had no significant impact on the kinetics of CTL induced apoptosis of target cells. It has recently been showed that as few as three specific peptide-MHC complexes need to be recognized to mediate CTL killing.¹⁸ Importantly, the recognition of so few pMHC complexes did not result in the establishment of a stable immunological synapse suggesting that only partial signalling is required for cytotoxic function CTL killing function.¹⁸ Given the low threshold of antigen required for eliciting cytotoxic function, it is no surprise that target cell death is independent from the duration of CTL contact.

While CTL mediated cytotoxicity only requires brief, low-density interactions,¹⁸ cytokine secretion requires sustained contact and TCR signalling.¹⁹ Therefore, while TCR avidity may not determine kinetics of target cell death, it is still possible that variation in pMHC/TCR avidity may still impact other functional differences. The high avidity D^bPA₂₂₄-specific CTL population recovered directly *ex vivo* shows higher levels of IFN- γ , TNF- α and IL-2 production following short-term *in vitro* stimulation with peptide.¹¹ Furthermore, differential levels of antigen availability may be a key factor in determining

the role of specific CTL during *in vivo* influenza virus infection. Earlier experiments²⁰ indicated that after infection, D^bNP₃₆₆ is expressed on the surface of a variety of cell types while D^bPA₂₂₄ is found only on dendritic cells. As such, differences in contact time observed between D^bNP₃₆₆- and D^bPA₂₂₄-specific CTL may reflect different roles during virus infection. It is tempting to suggest that while D^bPA₂₂₄-specific CTL are capable of mediating cytotoxicity,⁷ maybe their dominant role is helping establish an appropriate inflammatory environment by extended production of IFN- γ , TNF- α and IL-2 from prolonged contact with pMHC on dendritic cells.

By observing T cells in the time-lapse experiments, it was clear that, subsequent to elution from one target, virus-specific CTLs go on to find, and destroy additional cells expressing the appropriate pMHC complex (data not shown). Using both *in vitro* and *in vivo* cytotoxic assays, we have shown previously that D^bNP₃₆₆- and D^bPA₂₂₄-specific CTLs show the same level of cytotoxic capacity on a per cell basis.⁷ This analysis establishes that the lower-avidity D^bNP₃₆₆-specific CTL population can achieve the same level of target cell elimination as the D^bPA₂₂₄-specific set, but with shorter contact times; therefore, it is tempting to speculate that D^bNP₃₆₆-specific CTL may play a more significant role in ensuring viral clearance. This supports the observation that mutant influenza A viruses, lacking the NP₃₆₆ epitope, are more virulent in B6 mice.¹⁷ Furthermore, the ability of the D^bNP₃₆₆-specific effectors to elute more rapidly, and to potentially receive multiple stimulations, may be one of the several¹⁰ reasons why CTLs with this specificity are so prominent following secondary *in vivo* challenge.¹² As such, an overall profile of low, but sufficient, TCR/epitope avidity may thus be functionally advantageous and help to ensure efficient viral clearance after infection.

Materials and Methods

Generating CTLs by *in vitro* culture. Influenza-immune cells were recovered from the spleens of mice primed *i.p.* with the A/PR/8/34 H1N1 influenza A virus (PR8) influenza A virus 6 weeks earlier. Splenocytes from naive B6 mice were pulsed with 1 μ M of the OVA₂₅₇ or NP₃₆₆ peptide, or 10 nM PA₂₂₄ peptide for 1 h at 37 °C, irradiated (3000 rad from ⁶⁰Co source), and mixed with an equal number of B6-OT-I TCR transgenic or PR8-immune cells. These cultures were then maintained in c-RPMI (RPMI supplemented with 10% FCS/penicillin-streptomycin/200 mM L-glutamine/5 \times 10⁻⁵ M β 2-mercaptoethanol) for 7 days at 37 °C, 5% CO₂, stimulated again with peptide-pulsed irradiated splenocytes (as above), resuspended in c-RPMI, with 5 U/ml of recombinant human IL-2, and cultured for a further 5 days. Before time lapse imaging (see below), these *in vitro*-stimulated CTLs were FicolI-purified using lymphocyte separation medium (Cappel Laboratory, ICN Biomedicals, Seven Hills, New South Wales, Australia).

The *ex vivo* effectors. Secondary influenza-specific CTLs were generated by priming B6 mice *i.p.* with 1.5 \times 10⁷ PFU of the PR8 (H1N1) virus 6 weeks before intranasal challenge with 10⁴ PFU of the HK (H3N2) virus.¹⁵ The CTL effectors were then harvested by BAL after a further 8 days, and incubated on plastic six-well plates for 1 h at 37 °C, 5% CO₂, to remove adherent macrophages and monocytes.

Time-lapse microscopy. MC57 (H2^b) fibroblasts were plated at 1 \times 10⁴ cells per well in a 96-well plate and coated with 1 μ M of the appropriate peptide for 1 h at 37 °C before washing and adding 50 ng/ml PI and annexin V-FLUOS (2 μ g/ml). The plates were then maintained at 37 °C on the temperature-controlled stage (Prior Proscan; GT Vision) of a light fluorescence microscope (IX-81; Olympus). Equal numbers of effector CTLs were added to the targets, and images were captured at

specified intervals using a CCD camera (model ORCA-ER; Hamamatsu) controlled by MetaMorph software (Universal Imaging Corp.).⁴ To avoid the complication of individual targets receiving multiple hits from several effectors, only those encountering one CTL are shown in the analysis. Statistical significance was determined using an unpaired Student's *t*-test.

Tetramer elution to measure avidity. Lymphocyte populations (0.5–2 \times 10⁶ cells) were stained with the D^bNP₃₆₆-PE and D^bPA₂₂₄-PE tetramers for 1 h at room temperature, incubated with an mAb to H2D^b (50 μ g/ml) to prevent tetramer rebinding, and analysed by flow cytometry for tetramer loss over time.¹¹

Acknowledgements. This work was supported by an Australian Postgraduate Award to MRJ, a Burnet Award from the National Health and Medical Research Council of Australia (NHMRC) to PCD, RD Wright Fellowships from the NHMRC to NJW and NLG and a Pfizer Senior Research Fellowship to S.J.T. JAT is a senior principal research fellow of the NHMRC.

1. Topham DJ, Tripp RA, Doherty PC. CD8+ T cells clear influenza virus by perforin or Fas-dependent processes. *J Immunol* 1997; **159**: 5197–5200.
2. Lowin B, Peitsch MC, Tschopp J. Perforin and granzymes: crucial effector molecules in cytolytic T lymphocyte and natural killer cell-mediated cytotoxicity. *Curr Top Microbiol Immunol* 1995; **198**: 1–24.
3. Smyth MJ, Street SE, Trapani JA. Cutting edge: granzymes A and B are not essential for perforin-mediated tumor rejection. *J Immunol* 2003; **171**: 515–518.
4. Waterhouse NJ, Sutton VR, Sedelies KA, Ciccone A, Jenkins M, Turner SJ *et al*. Cytotoxic T lymphocyte-induced killing in the absence of granzymes A and B is unique and distinct from both apoptosis and perforin-dependent lysis. *J Cell Biol* 2006; **173**: 133–144.
5. Jenkins MR, Kedzierska K, Doherty PC, Turner SJ. Heterogeneity of effector phenotype for acute phase and memory influenza A virus-specific CTL. *J Immunol* 2007; **179**: 64–70.
6. Jenkins MR, Trapani JA, Doherty PC, Turner SJ. Granzyme K expressing CTL protect against influenza virus in granzyme AB^{-/-} mice. *Viral Immunol* 2008; **21**: 341–346.
7. Stambas J, Doherty PC, Turner SJ. An *in vivo* cytotoxicity threshold for influenza A virus-specific effector and memory CD8(+) T cells. *J Immunol* 2007; **178**: 1285–1292.
8. Turner SJ, Diaz G, Cross R, Doherty PC. Analysis of clonotype distribution and persistence for an influenza virus-specific CD8+ T cell response. *Immunity* 2003; **18**: 549–559.
9. Kedzierska K, Turner SJ, Doherty PC. Conserved T cell receptor usage in primary and recall responses to an immunodominant influenza virus nucleoprotein epitope. *Proc Natl Acad Sci USA* 2004; **101**: 4942–4947.
10. La Gruta NL, Doherty PC, Turner SJ. A correlation between function and selected measures of T cell avidity in influenza virus-specific CD8(+) T cell responses. *Eur J Immunol* 2006; **36**: 2951–2959.
11. La Gruta NL, Turner SJ, Doherty PC. Hierarchies in cytokine expression profiles for acute and resolving influenza virus-specific CD8+ T cell responses: correlation of cytokine profile and TCR avidity. *J Immunol* 2004; **172**: 5553–5560.
12. Belz GT, Xie W, Altman JD, Doherty PC. A previously unrecognized H-2D(b)-restricted peptide prominent in the primary influenza A virus-specific CD8(+) T-cell response is much less apparent following secondary challenge. *J Virol* 2000; **74**: 3486–3493.
13. Kedzierska K, La Gruta NL, Davenport MP, Turner SJ, Doherty PC. Contribution of T cell receptor affinity to overall avidity for virus-specific CD8+ T cell responses. *Proc Natl Acad Sci USA* 2005; **102**: 11432–11437.
14. Thomas PG, Keating R, Hulse-Post DJ, Doherty PC. Cell-mediated protection in influenza infection. *Emerg Infect Dis* 2006; **12**: 48–54.
15. Belz GT, Stevenson PG, Doherty PC. Contemporary analysis of MHC-related immunodominance hierarchies in the CD8+ T cell response to influenza A viruses. *J Immunol* 2000; **165**: 2404–2409.
16. Turner SJ, La Gruta NL, Stambas J, Diaz G, Doherty PC. Differential tumor necrosis factor receptor 2-mediated editing of virus-specific CD8+ effector T cells. *Proc Natl Acad Sci USA* 2004; **101**: 3545–3550.
17. Turner SJ, Kedzierska K, Komodromou H, La Gruta NL, Dunstone MA, Webb AI *et al*. Lack of prominent peptide-major histocompatibility complex features limits repertoire diversity in virus-specific CD8+ T cell populations. *Nat Immunol* 2005; **6**: 382–389.
18. Purbhoo MA, Irvine DJ, Huppa JB, Davis MM. T cell killing does not require the formation of a stable mature immunological synapse. *Nat Immunol* 2004; **5**: 524–530.
19. Valitutti S, Dessing M, Aktories K, Gallati H, Lanzavecchia A. Sustained signaling leading to T cell activation results from prolonged T cell receptor occupancy. Role of T cell actin cytoskeleton. *J Exp Med* 1995; **181**: 577–584.
20. Crowe SR, Turner SJ, Miller SC, Roberts AD, Rappolo RA, Doherty PC *et al*. Differential antigen presentation regulates the changing patterns of CD8+ T cell immunodominance in primary and secondary influenza virus infections. *J Exp Med* 2003; **198**: 399–410.

Supplementary Information accompanies the paper on Cell Death and Differentiation website (<http://www.nature.com/cdd>)